International Journal of Thermal Sciences 48 (2009) 1441–1451

Contents lists available at ScienceDirect

International Journal of Thermal Sciences

www.elsevier.com/locate/ijts

Applicability of calculation methods for conduction transfer function of building constructions

Xiang Qian Li [a,b], Youming Chen [a,b,*], J.D. Spitler [c], D. Fisher [c]

[a] College of Civil Engineering, Hunan University, Changsha, Hunan 410082, China
[b] Key Laboratory of Building Safety and Energy Efficiency, MOE, China
[c] School of Mechanical and Aerospace Engineering, Oklahoma State University, Stillwater, OK 74078-5016, USA

ARTICLE INFO

Article history:
Received 4 June 2008
Received in revised form 3 September 2008
Accepted 8 November 2008
Available online 6 December 2008

Keywords:
CTF coefficients
Error
Direct root-finding method
State-space method
Frequency-domain regression method

ABSTRACT

Conduction transfer function (CTF) is widely used to calculate conduction heat transfer in building cooling/heating loads and energy calculations. It can conveniently fit into any load and energy calculation techniques to perform conduction heat transfer calculations. There are three popular methods, direct root-finding (DRF) method, state-space (SS) method and frequency-domain regression (FDR) method to calculate CTF coefficients. The limitation of a methodology possibly results in imprecise or false CTF coefficients. This paper investigates the applicability of three methods as Fourier number and thermal structure factor are varied and in detail explains the sources that introduce error in the CTF solutions. The results show that the calculation error of SS and DRF methods becomes increasing as the reciprocal of the product of Fourier number and thermal structure factor becomes increasing. The maximal error even reaches almost 100%. However, the calculation error of FDR method always remains within 1% no matter how Fourier number and thermal structure factor are varied. Thus, FDR method is more robust and reliable than SS and DRF methods. And it is more practical to calculate CTF coefficients and may be a better choice to calculate the cooling/heating loads for building structures for the architect/designer.

1. Introduction

It becomes more and more important to predict energy and environment performance of building and heating, ventilation, and air conditioning (HVAC) system in their design, commissioning, operation and management [1], and to test and evaluate the control strategies and algorithm in Energy Management and Control Systems (EMCS) [2,3] by using simulation models. Models for space cooling/heating loads prediction (including weather data) are the most important part of building energy and HVAC system simulation programs. The heat transfer through building constructions is the principal component of space cooling/heating loads and energy requirements of a building [4]. For the purpose of detail evaluation of energy consumption and dynamic simulation of HVAC system, it is necessary to conduct transient thermodynamic analysis for heat flow in building constructions. This is because the massive elements of buildings in common use (e.g., concrete or brick walls) are rarely in steady state. The transient analysis of heat flow in buildings adds considerable complexity and computational expense to the building energy analysis and HVAC system dynamic simulation processes. The effort on developing better procedures for performing transient heat flow calculation has never stopped and the procedures are being improved without cease [5].

The response factor method and conduction transfer function (CTF) method are the most current approaches used widely for solving the heat conduction equation at present. CTF coefficients (CTFs) are a closed form representation of a conduction response factor series [6]. Stephenson and Mitalas [7] developed the response factor method to calculate the one-dimensional transient heat transfer through multi-layer walls, floors, and roofs. Kusuda [8] extended the response factor method to cylindrical and spherical coordinate systems. Stephenson and Mitalas [9] presented a method for determining transfer functions for one-dimensional heat transfer through multi-layer slabs by solving the conduction equation with Laplace and z-transform theory. Mitalas and Arsenault [10] wrote a program for computing transfer function coefficients based upon the method of Stephenson and Mitalas. Peavy [11] presented an alternative approach for calculating CTFs. Hittle [12] presented a very detailed derivation of transfer functions for multi-layer slabs which used the method of Peavy. In the well-known building energy and HVAC system simulation programs, the LOADS program simulator of DOE-2 computes heat gains and losses by conduction through building constructions using response factors [13–15]. BLAST uses both methods to make careful and complete analysis of transient heat conduction through walls [16,17]. HVACSIM+ [18], TRNSYS [19], IBLAST and EnergyPlus

* Corresponding author. Tel.: +86 731 8823515; fax: +86 731 8823515.
E-mail address: ymchen@hnu.cn (Y. Chen).

1290-0729/$ – see front matter
doi:10.1016/j.ijthermalsci.2008.11.006

Nomenclature

$\boldsymbol{a}, \boldsymbol{b}, \boldsymbol{c}, \boldsymbol{d}$	coefficient matrices
$A(s), B(s), D(s)$	overall transmission matrix elements
a_m	thermal diffusivity ... m^2/s
C	thermal capacity
c_p	specific heat ... J/(kg K)
f	decrement factor, dimensionless
G	polynomial s-transfer functions
j	imaginary number unit
k	thermal conductivity ... W/(m K)
L	thickness ... m
n	number of layers
N_x, N_y, N_z	number of exterior, cross and interior CTF terms
N_φ	number of flux history terms
q	heat flux ... W/m^2
Q	flux history term ... W/m^2
r	orders of the numerator
R	thermal resistance of film coefficient ... $(m^2 K)/W$
$R_{i\text{-}m}$	resistance from the surface of layer m to inner surrounding ... $(m^2 K)/W$
$R_{m\text{-}o}$	resistance from the surface of layer m to outer surrounding ... $(m^2 K)/W$
s	Laplace transfer variable
S_{ie}	thermal structure factor, dimensionless
T	temperature ... °C
T_A	amplitude of the sinusoidal temperature variation . °C
U	overall heat transfer coefficient ... $W/(m^2 K)$
x	heat flow direction ... m
X_k, Y_k, Z_k	exterior, cross and interior CTF coefficient $W/(m^2 K)$

Greek symbols

α_v, β_r	real coefficients
$\Delta\tau$	time interval ... s or h
φ_k	flux coefficient, dimensionless
v	orders of the denominator
ρ	density ... kg/m^3
τ	time ... s
ψ	time lag ... hour
ω	frequency ... s^{-1}

Subscripts

i	inside or interior
o	outside or exterior
s	surface
T	total
θ	current time
δ	time step

[15,20] adopt CTFs to evaluate the heat gains and losses through building constructions.

In these building simulation programs, the dynamic thermal behavior data of building constructions including thermal response factors, CTFs or periodic response factors are calculated by various algorithms, and then utilized in conjunction with weather data to calculate the heat flow through the constructions [21]. The accuracy of the dynamic thermal behavior data directly affects the accuracy of the building loads and/or energy calculations. However, there are various potential factors such as the limitation of calculation methods, too big iteration step, low calculation precision, unconverged computational results, etc., which may lead to incorrect results in calculating the dynamic thermal behavior data. As pointed out by Spitler and Fisher [6], computational inaccuracy sometimes occurs in calculating the dynamic thermal behavior data. All the factors can result in that the computational building cooling/heating loads are either more or less than the actual building cooling/heating loads. Thus, the architect/designer determines the uneconomical design or retrofit based upon inappropriate heating, cooling, equipment, and material costs. In addition, the size of HVAC equipment, determined by estimating peak heating/cooling loads for buildings, will be also inappropriate. Over sizing HVAC equipment results in excessive capital cost for equipment and extra energy consumption due to inefficient part-load operation of equipment. Under sizing HVAC equipment results in uncomfortable indoor environment [22]. Moreover, it is rather difficult to be developed that optimal control strategies which minimize HVAC operating costs while maintaining a comfortable environment for the occupants. Therefore, in order to provide accurate space cooling/heating loads of buildings for the architect/designer, it is necessary to seek a precise and high efficient calculation method for dynamic thermal behavior solution.

In cooling load and energy calculation, building simulation as well as energy analysis, conduction heat transfer is usually modeled as a one-dimensional, transient process with constant material properties [23]. The simplified heat diffusion equation [24] in Cartesian coordinates is shown in Eq. (1).

$$\frac{\partial^2 T(x,\tau)}{\partial x^2} = \frac{1}{a_m}\frac{\partial T(x,\tau)}{\partial \tau} \tag{1}$$

where T, x, a_m and τ are the temperature, heat flow direction, thermal diffusivity and time, respectively.

Fourier's law, Eq. (2), specifies the conduction heat flux in terms of the thermal conductivity of the material and temperature gradient across a differential thickness.

$$q = -k\frac{\partial T(x,\tau)}{\partial x} \tag{2}$$

where q is heat flux and k is thermal conductivity.

Since Eq. (1) is a partial differential equation, the system is usually solved numerically, often by means of CTF method. CTFs represent the material's thermal response as determined by its material properties. The method results in a simple linear equation that expresses the current heat flux in terms of the current temperature and temperature and heat flux histories. The linear form of Eqs. (3) and (5) greatly reduce the required computational effort compared to other numerical techniques and facilitates computer implementation of the CTF method.

The CTF formulation of the surface heat fluxes involves four sets of coefficients. Following the nomenclature in the literature [23] X, Z, and Y are used to represent the exterior, interior and cross terms respectively. Eq. (3) shows the zeroth exterior and cross terms operating on the current hour's surface temperatures. Q_o is the exterior flux history term as shown in Eq. (4). Together the current hour's surface temperatures and the history term yield the total flux at the exterior surface.

$$q_{o,\theta} = -Y_0 T_{is,\theta} + X_0 T_{os,\theta} + Q_o \tag{3}$$

$$Q_o = -\sum_{k=1}^{N_y} Y_k T_{is,\theta-k\delta} + \sum_{k=1}^{N_x} X_k T_{os,\theta-k\delta} + \sum_{k=1}^{N_\varphi} \varphi_k q_{o,\theta-k\delta} \tag{4}$$

Likewise, Eqs. (5) and (6) show the flux at the interior surface.

$$q_{i,\theta} = -Z_0 T_{is,\theta} + Y_0 T_{os,\theta} + Q_i \tag{5}$$

$$Q_i = -\sum_{k=1}^{N_z} Z_k T_{is,\theta-k\delta} + \sum_{k=1}^{N_y} Y_k T_{os,\theta-k\delta} + \sum_{k=1}^{N_\varphi} \varphi_k q_{i,\theta-k\delta} \tag{6}$$

where q_o and q_i are heat flux at exterior and interior surfaces, respectively. X_k, Y_k and Z_k are exterior, cross and interior CTFs, respectively. T_{is} and T_{os} are the interior and exterior surface temperature, respectively. N_x, N_y and N_z are number of exterior, cross and interior CTFs terms, respectively. ϕ_k is the flux coefficient. N_ϕ is the number of flux history terms. The subscript θ represents the current time, and δ is time step.

As indicated in Eqs. (3) and (5), the current heat fluxes are closely related to the flux histories. The flux histories, shown as constant terms in Eqs. (3) and (5), are not only related to previous surface temperatures, but are also related to previous heat fluxes. Eqs. (3) and (4) or (5) and (6) are usually solved iteratively with an assumption that all previous heat fluxes are equal at the beginning of the iteration. The converged solution produces flux history terms (Q_o and Q_i) that account for the thermal capacitance of a given construction. For light weight materials, the thermal response is fast and a few history terms are enough to accurately calculate the current heat flux, while for heavy weight materials, more terms are needed. Since CTFs are temperature independent, they are usually calculated during program initialization and may be saved in a library or database. Pre-calculated CTFs of some typical constructions are available in the literatures [25,26].

While there are a number of numerical methods to calculate CTFs by solving Eqs. (1) and (2), direct root-finding (DRF) method and state-space (SS) method are the most widely used in cooling loads and energy calculations. Frequency-domain regression (FDR) method is developed recently as another alternative method. This paper investigates the applicability of three methods through comparing the calculation error of three methods as Fourier number and thermal structure factor are varied. Fourier number and thermal structure factor are introduced to represent the thermal characteristic of the building slabs. They will be changed when the layer thickness, specific heat, density and thermal conductivity are changed. Single-layered and multi-layered building constructions are taken as calculating examples. The detailed description of three methods is shown as Section 2.

2. Overview of calculating methods for CTF

2.1. Direct root-finding method

Hittle [27] introduced a procedure to solve the conduction heat transfer governing equations (1) and (2) by using direct root-finding (DRF) method. The system in the Laplace domain is shown in Eq. (7).

$$\begin{bmatrix} q_i(s) \\ q_o(s) \end{bmatrix} = \begin{bmatrix} \frac{D(s)}{B(s)} & \frac{-1}{B(s)} \\ \frac{1}{B(s)} & \frac{-A(s)}{B(s)} \end{bmatrix} \begin{bmatrix} T_i(s) \\ T_o(s) \end{bmatrix} \tag{7}$$

where $A(s)$, $B(s)$ and $D(s)$ are overall transmission matrix elements that depend on material properties, and/or air film coefficients.

Response factors are generated by applying a unit triangular temperature pulse to the inside and outside surface of the multi-layered slab as shown in Fig. 1. The response factors are defined as the discretized heat fluxes on each surface due to both the outside and inside temperature pulse. The response factors are an infinite series. In the calculation of response factor or CTFs, a numerical search for the roots of a nonlinear equation must be performed. Hittle and Bishop [28] developed an improved numerical technique for calculating the roots of the nonlinear equation. Hittle [27] also described an algebraic operation to group response factors into CTFs, and to truncate the infinite series of response factors by the introduction of flux histories coefficients. A convergence criterion shown in Eq. (8) is used to determine whether the numbers of CTFs and flux history terms are sufficient such that the resulting CTFs accurately represent the response factors. Therefore, through Laplace inverse transform of transfer functions $D(s)/B(s)$, $-1/B(s)$ and $-A(s)/B(s)$ with unit triangle temperature pulse, response factors and CTFs can be worked out.

$$\sum_{k=0}^{N_x} X_k = \sum_{k=0}^{N_y} Y_k = \sum_{k=0}^{N_z} Z_k = U\left(1 - \sum_{k=1}^{N_\varphi} \varphi_k\right) \tag{8}$$

where U is the overall heat transfer coefficient of a building slab.

2.2. State-space method

A state-space (SS) formulation has traditionally been used to analyze linear systems which may have many inputs and outputs. A heat transfer problem may be formulated in a SS representation by using finite-difference or finite-element methods [29] to

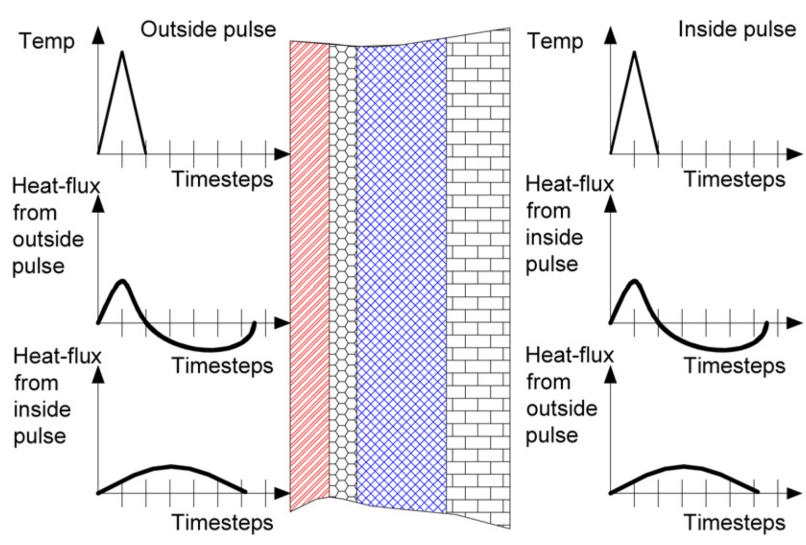

Fig. 1. The generation of response factors.

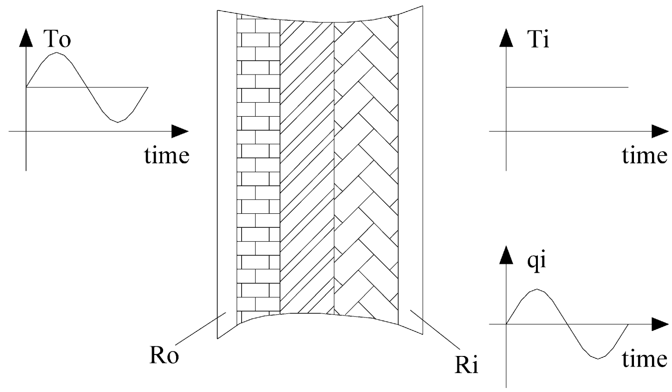

Fig. 2. CTF test procedure scheme.

spatially discretize the problem. The use of SS method by solving the governing equations (1) and (2) was introduced in literatures [22,30–32]. The SS expression relates the interior and exterior boundary temperatures to the inside and outside surface heat fluxes at each node of a multi-layered slab as shown in Eqs. (9) and (10).

$$\begin{bmatrix} \frac{dT_1}{dt} \\ \frac{dT_2}{dt} \\ \vdots \\ \frac{dT_n}{dt} \end{bmatrix} = \boldsymbol{a} \begin{bmatrix} T_1 \\ T_2 \\ \vdots \\ T_n \end{bmatrix} + \boldsymbol{b} \begin{bmatrix} T_i \\ T_o \end{bmatrix} \tag{9}$$

$$\begin{bmatrix} q_i \\ q_o \end{bmatrix} = \boldsymbol{c} \begin{bmatrix} T_1 \\ T_2 \\ \vdots \\ T_n \end{bmatrix} + \boldsymbol{d} \begin{bmatrix} T_i \\ T_o \end{bmatrix} \tag{10}$$

where $T_1, T_2, \ldots, T_n$ is the temperature of each node. $\boldsymbol{a}, \boldsymbol{b}, \boldsymbol{c}, \boldsymbol{d}$ are coefficient matrices that depend on material properties, and/or air film coefficients.

Coefficients matrices $\boldsymbol{a}, \boldsymbol{b}, \boldsymbol{c}, \boldsymbol{d}$ can be worked out through numerical computation. And then the CTFs can be obtained by Leverrier's algorithm [33] from coefficients matrices $\boldsymbol{a}, \boldsymbol{b}, \boldsymbol{c}, \boldsymbol{d}$.

2.3. Frequency-domain regression method

The use of frequency-domain regression (FDR) method to calculate CTFs by solving the governing equations (1) and (2) was introduced by Chen, et al. [34]. Based on Laplace transform, transmission matrix of a single-layered slab can be obtained. The frequency characteristics of interior, cross and exterior heat transfer of a multi-layered slab are calculated through transmission matrix multiplication by substituting s with $j\omega$ (where $j = \sqrt{-1}$). It is very easy to calculate the frequency characteristics of a multi-layered slab. FDR method is used to estimate some simple s-transfer functions in the form of Eq. (11) from the interior, cross and exterior frequency characteristics.

$$G(s) = \frac{\beta_0 + \beta_1 s + \beta_2 s^2 + \cdots + \beta_r s^r}{1 + \alpha_1 s + \alpha_2 s^2 + \cdots + \alpha_v s^v} \tag{11}$$

where α_v and β_r are real coefficients. r and v are the orders of the numerator and denominator.

The simple s-transfer functions are in the forms of the polynomial ratio of variable s. They are called polynomial s-transfer functions. In FDR method, by minimizing the sum of the square error between the frequency characteristics of the multi-layered slab and the polynomial s-transfer function at all frequency points, the coefficients of the polynomial s-transfer function are easily obtained by solving a set of linear equations. The frequency characteristic of the polynomial s-transfer functions is also evaluated by substituting s with $j\omega$. Through Laplace inverse transform of interior, cross and exterior transfer functions $G(s)$ with unit triangle temperature pulse, response factors and CTFs can be worked out.

3. Accuracy verification for CTFs and test procedure

A conventional CTFs verification is to check whether or not they give the correct heat transfer in steady-state as shown in Eq. (12).

$$\frac{\sum_{k=0}^{N_x} X_k}{(1 - \sum_{k=1}^{N_\varphi} \varphi_k)} = \frac{\sum_{k=0}^{N_y} Y_k}{(1 - \sum_{k=1}^{N_\varphi} \varphi_k)} = \frac{\sum_{k=0}^{N_z} Z_k}{(1 - \sum_{k=1}^{N_\varphi} \varphi_k)} = U \tag{12}$$

The above relationships are valid for the case when frequency ω is 0, but do not address the accuracy for dynamic thermal behavior.

There is a method [4] for the verification of dynamic CTFs, based on the equivalence of the frequency characteristics between a linear system and its dynamic model. The Bode diagrams for a linear system, i.e., the amplitude-frequency and phase-frequency curves depicting the frequency characteristics of the system, can be used as visual aids to judge whether or not the dynamic model is consistent with the described system. Thereby we can verify the CTFs to judge the agreement of the frequency characteristics of the system and its model.

The heat flux comparison method is employed here. This method verifies the accuracy of CTFs by checking difference between heat flux calculated by CTF method and analytical solution. The analytical solution is explained as follows:

The conduction governing equations (1) and (2) are usually not solved analytically in building thermal load and energy calculations primarily due to the computational intensity of the implementation. However, with a periodic temperature boundary condition on one side of the slab and a constant temperature boundary condition on the other side, the analytical solution is tractable. Spitler et al. [35] presented an analytical solution for a multi-layered slab subject to a sinusoidal outside temperature and a constant inside temperature, as shown in Fig. 2. For single-layered slabs, the inside temperature and heat flux are related to the outside temperature and heat flux by the following set of equations:

$$\begin{bmatrix} T_i \\ q_i \end{bmatrix} = \begin{bmatrix} m_1 & m_2 \\ m_3 & m_1 \end{bmatrix} \begin{bmatrix} T_o \\ q_o \end{bmatrix} \tag{13}$$

where $m_1 = \cosh(p + jp)$ (14)

$$m_2 = \frac{L \sinh(p + jp)}{k(p + jp)} \tag{15}$$

$$m_3 = \frac{k(p + jp)\sinh(p + jp)}{L} \tag{16}$$

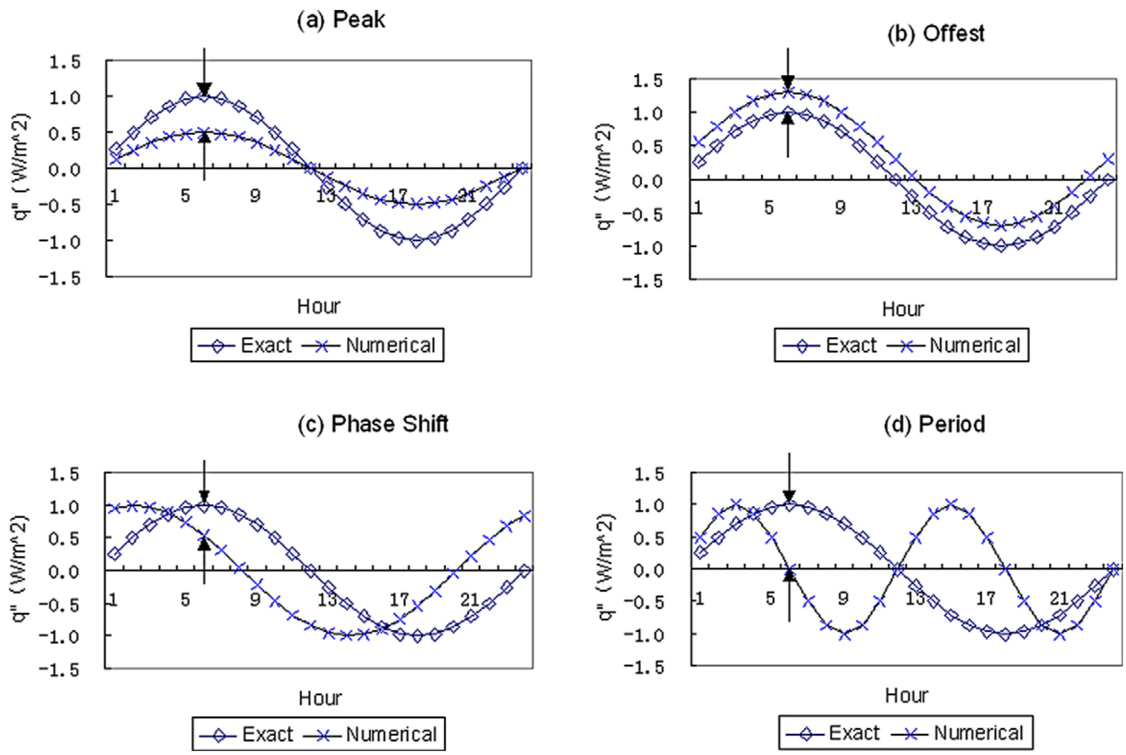

Fig. 3. Error types and measure in the CTF solution test (arrows indicate error).

$$\text{for a 24-hour cycle} \quad p = \left(\frac{\pi L^2 \rho c_p}{86400k}\right)^{0.5} \tag{17}$$

$$j^2 = -1 \tag{18}$$

where L, ρ and c_p are thickness, density and specific heat, respectively.

For a resistive layer, Eqs. (14) to (16) can be simplified as follows:

$$m_1 = 1 \tag{19}$$

$$m_2 = R \tag{20}$$

$$m_3 = 0 \tag{21}$$

The matrix formulation shown in Eq. (13) can be extended for multi-layered slabs with appropriate changes on the m matrix, shown in Eq. (22).

$$\begin{bmatrix} T_i \\ q_i \end{bmatrix} = \begin{bmatrix} M_1 & M_2 \\ M_3 & M_1 \end{bmatrix} \begin{bmatrix} T_o \\ q_o \end{bmatrix} \tag{22}$$

where

$$\begin{bmatrix} M_1 & M_2 \\ M_3 & M_1 \end{bmatrix} = \begin{bmatrix} 1 & R_i \\ 0 & 1 \end{bmatrix} \begin{bmatrix} m_1 & m_2 \\ m_3 & m_1 \end{bmatrix}_{\text{layer},1} \begin{bmatrix} m_1 & m_2 \\ m_3 & m_1 \end{bmatrix}_{\text{layer},2} \cdots \begin{bmatrix} m_1 & m_2 \\ m_3 & m_1 \end{bmatrix}_{\text{layer},n} \begin{bmatrix} 1 & R_o \\ 0 & 1 \end{bmatrix} \tag{23}$$

where n is the layer number of a slab. R_i and R_o are the thermal resistance of inside and outside air film coefficients, respectively.

As a result, the so-called decrement factor f and time lag ψ can be calculated as follows:

$$f = \left|\frac{1}{UM_2}\right| \tag{24}$$

$$\psi = -\frac{1}{\omega}\tan^{-1}\left[\frac{\mathrm{Im}\left(\frac{1}{UM_2}\right)}{\mathrm{Re}\left(\frac{1}{UM_2}\right)}\right] \tag{25}$$

where ω is the frequency of temperature boundary condition. The arctangent should be evaluated in the range of $-\pi$ to 0 radians.

For a sinusoidal outside temperature and a constant inside temperature, the inside heat flux can be formulated as:

$$q_i(\tau) = UfT_A \sin[\omega(\tau - \psi)] \tag{26}$$

where T_A is the amplitude of the sinusoidal temperature variation.

The heat flux calculated from Eq. (26) is thus the exact solution of Eqs. (1) and (2) for a sinusoidal outside temperature and a constant inside temperature. If conduction is the only heat transfer in a control volume, and with constant inside and outside film coefficients, Eq. (26) can be used to calculate the exact cooling load values. The test procedure uses the analytical solution to benchmark the accuracy of conduction calculations by SS, DRF and FDR CTFs.

The error is calculated as the percent deviation of the numerical, CTF calculated heat flux from the analytical solution as follows:

$$error = \frac{q_{\text{num}} - q_{\text{exact}}}{q_{\text{exact}}} \times 100\% \tag{27}$$

where q_{exact} is the peak value of the 24-hour conduction heat fluxes calculated from analytical solution, q_{num} is the conduction heat flux calculated by CTFs at the same time as q_{exact}. Fig. 3 shows how the error values are measured in the test. If CTF numerical and application errors exist in the conduction calculation, any of the error characteristics shown in Fig. 3, or a combination of them could exist in the CTF solution.

In the test, ASHRAE Loads Toolkit (2001) algorithm [26] was used to calculate SS and DRF CTF solutions. The procedure adopts the default Toolkit CTF algorithm settings (Table 1). FDR FORTRAN codes come from the translation of FDR MATLAB codes [36]. Fig. 2 illustrates the boundary conditions and the calculated result of the test procedure. The inside and outside film coefficients are treated as resistive layers and the resistances R_i and R_o are respectively equal to 0.120 and 0.044 ($\mathrm{m^2\,K}$)/W. The steady, 24-hour periodic outside temperature, T_o is shown on the left-hand side of the figure. The constant inside temperature, T_i, and the resulting inside

Table 1
Default Toolkit settings for CTF solution.

Error types	Error sources	Parameter settings	
		SS CTF	DRF CTF
CTF numerical error	(a) No. of SS nodes	10–19 per layer Total no. of nodes $\leqslant$ 75	NA
	(b) Root finding tolerance	NA	1E–12–1E–10 No. of roots found $\leqslant$ 60
	(c) No. of CTF terms	TL is 1E–13 Total no. of CTFs $\leqslant$ 19	TL is 1E–13 Total no. of CTFs $\leqslant$ 19
	(d) Solution time step	1 hour	1 hour
Application error	(e) Solution convergence*	TL is 1E–6 and NI is 100	TL is 1E–6 and NI is 100
	(f) No. of flux history terms	24	24

Note: NA is Not applicable.
TL is tolerance.
NI is no. of iterations.
*is User defined parameters.

surface heat flux are shown on the right-hand side. The sinusoidal outside air temperature profile is approximated for 1-hour time steps and 24-hour period as shown in Eq. (28). The inside air temperature is the mean air temperature, T_m.

$$T_o = T_m + T_A \sin\left(\frac{\pi}{12}\tau\right) \tag{28}$$

The mean air temperature is 20 °C, and the amplitude temperature is also 20 °C. The material properties and number of layers of the slab are varied over a wide range in order to investigate the range of applicability of the three CTF calculation methods.

4. Wall structure characteristic parameter

To show the relationship between the wall material fabric and the CTFs calculation error, Fourier number and thermal structure factor are introduced here.

Fourier number is defined as Eq. (29):

$$Fo = \frac{\Delta\tau}{RC} \tag{29}$$

$$R = \frac{L}{k} \tag{30}$$

$$C = L\rho c_p \tag{31}$$

Since the time step $\Delta\tau$ is constant in the CTF calculations, changes in the Fourier number represent changes in material properties only. Eq. (29) shows that Fourier numbers for heavy weight materials (larger thermal capacity C) are smaller than those for light weight materials. In other words, the value of $1/Fo$ is larger for heavy weight materials. As the layer thickness (L), specific heat (c_p), density (ρ) increasing and thermal conductivity (k) decreasing, the reciprocal of Fourier number is increasing. Meantime, the slab becomes more thermally massive. Thus, Fourier numbers can be used for representing the heavyweight characteristic of the slabs.

However, the relationship between $1/Fo$ and CTF solution errors shown above is only suitable for single-layered slabs. For multi-layered slabs, not only material properties, but the layer arrangement also influences CTF calculations. In order to take the layer arrangement into account, thermal structure factor [37] is introduced. Thermal structure factor of a multi-layered slab is determined by both thermal characteristic parameters and arrangement of structure layers. It incorporates all these affecting factors into unity index. To demonstrate the effect of layers arrangement sequence on thermal structure factors, Kossecka examined six simple examples in the literature [37]. Those results show that thermal structure factor is an appropriate parameter describing the wall structure character.

The thermal structure factor S_{ie} is related to thermal resistance and capacity as shown below, where layer 1 is the interior layer.

$$S_{ie} = \frac{1}{R_T^2 C_T}\sum_{m=1}^{n} C_m\left(-\frac{R_m^2}{3} + \frac{R_m R_T}{2} + R_{i\text{-}m}R_{m\text{-}o}\right) \tag{32}$$

$$R_{i\text{-}m} = R_i + \sum_{k=1}^{m-1} R_k \tag{33}$$

$$R_{m\text{-}o} = R_o + \sum_{k=m+1}^{n} R_k \tag{34}$$

where n is the number of slab layers. R_i and R_o are thermal resistance of inside and outside film coefficient, respectively. R_T and C_T are total thermal resistance and capacity, respectively. R_m and R_k are thermal resistances of the mth, kth slab layer, respectively, and C_m is thermal capacity of the mth slab layer.

For single-layered slab, thermal structure factor can be simplified as:

$$S_{ie} = \frac{1}{6} + \frac{R_i R_o}{R^2} \tag{35}$$

For taking Fourier number and thermal structure factor into account, $1/(FoS_{ie})$ is taken as the wall structure characteristic parameter here.

5. Comparisons and discussions

5.1. Single-layered slab

The test procedure starts with a single-layered slab described in Table 2. It is ASHRAE (2001) [26] wall 24. The slab is subject to the changes of layer thickness (L), thermal conductivity (k), density (ρ) and specific heat (c_p) respectively until the CTF solutions fail to converge. When one property of the slab changes proportionally, the other properties keep unchanged. Table 3 gives an example of thickness changing based on ASHRAE wall 24.

Fig. 4 shows that the errors of SS and DRF solutions remain within 5% as $1/(FoS_{ie})$ are less than 600 (for example, $L = 0.4877$ m). The error can be accepted. As $1/(FoS_{ie})$ increasing, the errors of SS solution appear proportionally increasing tendency, while one of DRF solution is stable. When $1/(FoS_{ie})$ are more than 600, i.e., material properties become very more thermally massive, the errors of SS and DRF solutions are wide-range increasing and even reach almost 100%. The maximum error value

Table 2
Details of ASHRAE wall 24.

Description	Thickness and thermal properties				
	L [m]	K [$\mathrm{Wm^{-1}\,K^{-1}}$]	P [$\mathrm{kg\,m^{-3}}$]	c_p [$\mathrm{J\,kg^{-1}\,K^{-1}}$]	R [$\mathrm{m^2\,K\,W^{-1}}$]
Outside surface film	–	–	–	–	0.044
LW concrete block (filled)	0.2032	0.26	465	879	0.783
Inside vertical surface film	–	–	–	–	0.120

Table 3
Structure factor and CTF error with proportionally-changing thickness.

Changing scale		...	−0.30	−0.20	−0.10	0.00	0.10	0.20	0.30	...
L (m)*		...	0.1422	0.1626	0.1829	0.2032(L_0)	0.2235	0.2438	0.2642	...
$1/(FoS_{ie})$		...	47.993	64.117	82.440	102.951	125.641	150.507	177.546	...
Error	SS (%)	...	−0.5869	−0.6639	−0.6399	−0.7683	−0.7127	−0.8983	−1.1408	...
	DRF (%)	...	−0.5868	−0.5661	−0.6001	−0.5725	−0.5922	−0.5742	−0.5821	...
	FDR (%)	...	−0.5641	−0.5654	−0.5678	−0.5698	−0.5704	−0.5702	−0.5698	...

Note: $^*L = L_0 \times (1 + \text{Changing scale})$.

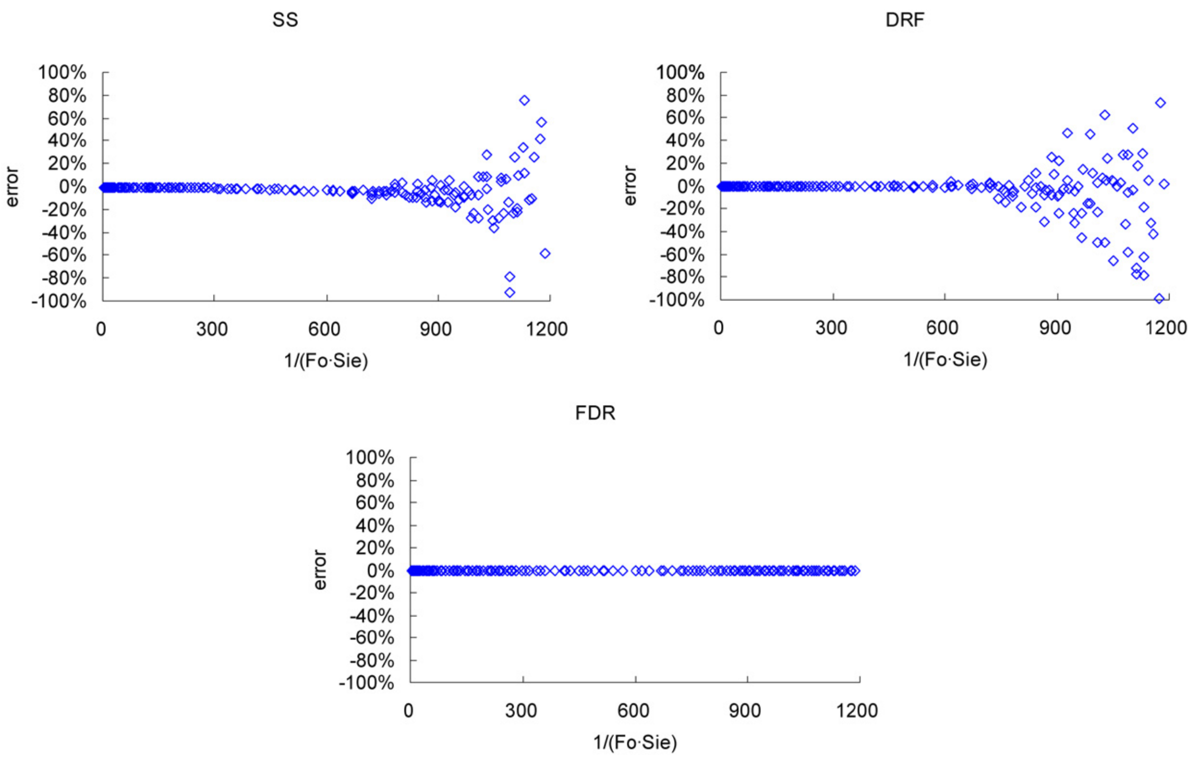

Fig. 4. Single-layered CTF solution errors.

is −92.5% for SS solution, and is −99.38% for DRF solution. The hourly heat flux profiles at the large errors are shown in Fig. 5. Such large errors are unaccepted. However, for the case of FDR solution, no matter whether the slabs are lightweight or heavyweight and no matter how $1/(FoS_{ie})$ is varied, the errors of FDR solution always remain within 1%. Therefore, for single-layered slabs, the calculation precision of FDR solution is higher and the calculation range is more comprehensive than SS and DRF solutions.

5.2. Multi-layered slabs

Since the maximum number of layers is limited to 10 in the Toolkit algorithm including the inner and outer layers used to model the surface film resistances, a wall with eight layers is considered here for test. ASHRAE (2001) [26] wall 19 is investigated and the wall is described in Table 4. Both brick layer and heavyweight concrete layer of the wall are simultaneously subject to the changes of layer thickness (L), thermal conductivity (k), density (ρ) and specific heat (c_p) respectively until the CTF solutions fail to converge. The material properties are changed as the single-layered slab case.

Fig. 6(a) shows CTF solution errors for wall 19. The errors of SS and DRF solutions remain within 5% as $1/(FoS_{ie})$ are less than 1200 (for example, $L = 0.2743$ m for the heavyweight concrete layer and $L = 0.0914$ m for the brick layer). The error can be accepted. As $1/(FoS_{ie})$ increasing, the errors of SS solution appear proportionally increasing tendency, while one of DRF CTF solution is stable. When $1/(FoS_{ie})$ are more than 1200, i.e., the material properties become very more thermally massive, the errors of SS and DRF solutions are wide-range increasing and even reach almost 100%. The results are quite consistent with the single-layered case.

Fig. 6(b) shows the error results for the wall 19 exchanged the arrangement sequence of the brick layer and heavyweight concrete

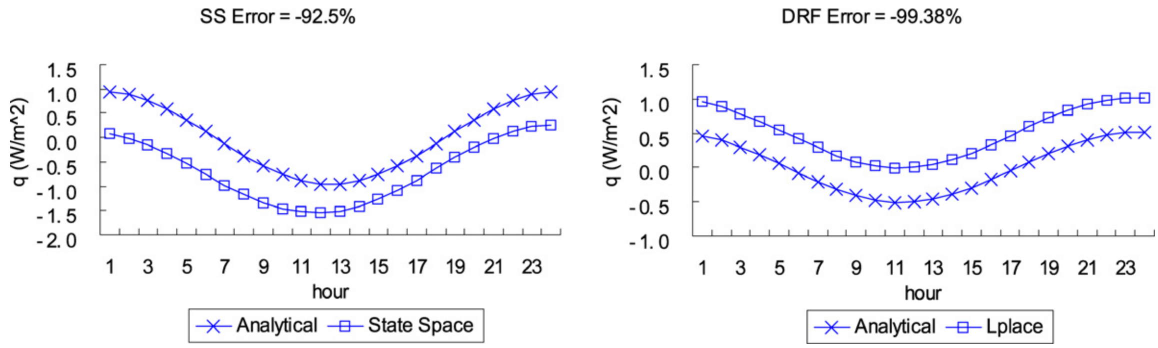

Fig. 5. Maximum errors in the single slabs test.

Table 4
Details of ASHRAE wall 19.

Description	Thickness and thermal properties				
	L [m]	K [$\mathrm{W\,m^{-1}\,K^{-1}}$]	ρ [$\mathrm{kg\,m^{-3}}$]	c_p [$\mathrm{J\,kg^{-1}\,K^{-1}}$]	R [$\mathrm{m^2\,K\,W^{-1}}$]
Outside surface film	–	–	–	–	0.044
Brick	0.1016	0.894	1922.2	795.5	0.114
Wall air space resistance	–	–	–	–	0.153
Insulation board	0.0254	0.029	43.2	1214.2	0.881
Heavyweight concrete	0.3048	1.947	2242.6	921.1	0.157
Wall air space resistance	–	–	–	–	0.153
Gyp board	0.0159	0.160	800.9	1088.6	0.099
Inside vertical surface film	–	–	–	–	0.120

layer. Obviously, comparing Fig. 6(b) with Fig. 6(a), SS and DRF solutions errors decrease rapidly in a specific value of $1/(FoS_{ie})$, such as from 1200 to 2000, i.e., calculation ranges of SS and DRF solutions become much larger. The results indicate apparently that it is very necessary and feasible to introduce thermal structure factor to express the wall structure parameter.

Fig. 6 also show that the errors of FDR solution always remain within 1% no matter how $1/(FoS_{ie})$ are changed and conditions are varied. As shown in the examples of wall 19 and 24, FDR method is more applicable and accuracy than SS and DRF methods. FDR method may be a better choice to calculate CTFs for the buildings simulation programs.

6. Sources of error in CTF solution

Since CTFs are the products of numerical solution, numerical error exists in the CTF solution. The errors come from the solution used in solving the transient conduction equations. As the numerical methods: DRF, SS and FDR methods, are concerned, the error sources are categorized as follows:

- **Root finding tolerance and missed roots:** This error applies only to DRF method. In order to calculate response factors, it is necessary to find the root of $B(s) = 0$ in Eq. (7) [27]. Since the expression for $B(s)$ becomes complicated for the slabs with more than one layer, the root finding procedures rely on numerical method. The procedures iteratively continue until the root is found within a root finding tolerance or the maximum number of iterations is reached. The tolerance value and number of iterations can cause error in the CTF calculation. For a multi-layered heavyweight construction, there is a risk of missing several roots in the numerical search, especially in case where two adjacent roots are close together. The large DRF error values in Figs. 4 and 6 indicate right the missed roots error. Table 5 shows the relationship between the CTFs accuracy and root finding tolerance only when the thickness L of wall 24 is changed. The result indicates that errors are less when root finding tolerance is adopted appropriately.
- **Ill-conditioned or near-singular matrix:** This error applies only to SS method that uses state equations with matrices to represent the relationship between the inputs and outputs in heat transfer system through a building construction. The numerical computation for CTFs involves the integration and inversion of a large matrix. For a multi-layered heavyweight construction, the state matrix possibly is ill-conditioned or near-singular. An ill-conditioned or near-singular state matrix will result in inaccurate CTFs.
- **Number of nodes:** This error applies only to SS method that uses SS nodes to discretize the transient conduction equations. Seem [22] demonstrated that the CTFs accuracy is dependent on the number of nodes specified. The CTFs accuracy is proportional to the number of nodes used in each material layer in the calculation. Thus, the number of nodes can cause error in the CTF calculation. Table 6 shows the relationship between the CTFs accuracy and the number of nodes only when the thickness L of wall 24 is changed. The results reveal that the calculation becomes more accurate with the increased number of nodes.
- **Number of CTF terms:** In DRF method, CTFs are derived from response factors and it is necessary to determine the number of CTF terms so that the resulting CTFs can equivalently represent the response factors. Eq. (8) is used to check the equivalence of response factors and CTFs. While in SS method, the number of CTF terms is determined by tracking the ratio of the last CTF flux term to the first term until the value is negligible [22]. The number of CTF terms is determined with an iterative process until the conditions are satisfied within a tolerance limit or until the maximum number of iterations is reached. The tolerance value and number of iterations can introduce errors in the CTF calculation. Table 7 shows that the CTFs calculation accuracy is rather sensitive to the tolerance value to determine the number of CTF terms based on wall 24.
- **Solution time step:** CTFs are calculated based on an assumed temperature boundary condition. In the CTF calculation, the temperature variation is divided into time steps where the subset of temperature variation is approximated with linear temperature profiles. Therefore, this error is apparent when

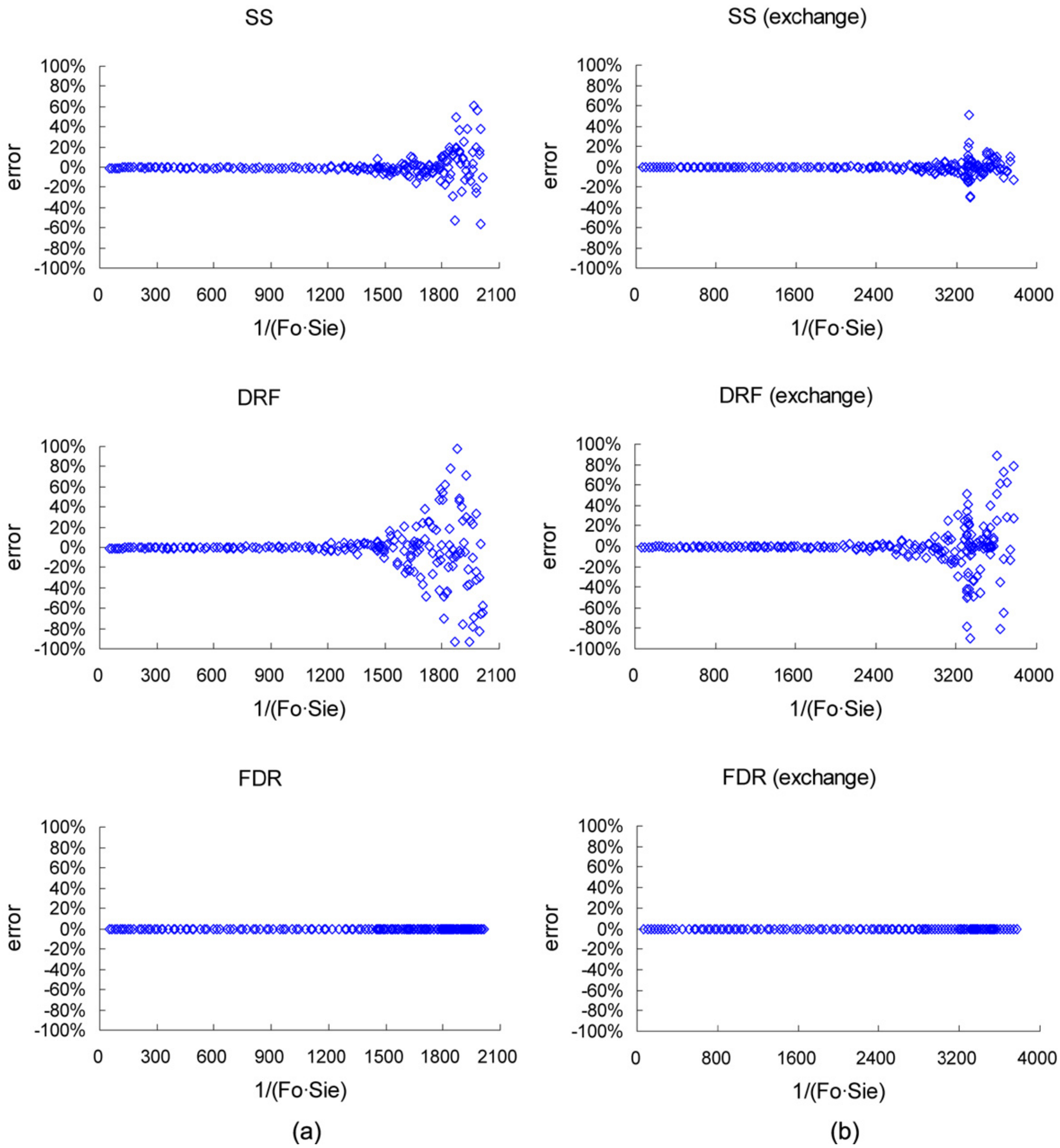

Fig. 6. 6-layered CTF solution errors.

Table 5
Relationship between CTFs accuracy and root finding tolerance.

$L = 0.5283$ m	Tolerance	1.0E–04	1.0E–07	1.0E–10	1.0E–13
	DRF error	−0.22%	−0.19%	−0.33%	0.03%
$L = 0.5812$ m	Tolerance	1.0E–06	1.0E–07	1.0E–08	1.0E–09
	DRF error	−5.61%	−5.43%	−4.89%	−4.16%

Table 6
Relationship between CTFs accuracy and SS nodes.

$L = 0.2845$ m	Nodes	4	5	6	7	8	9
	Total nodes	11	14	17	20	23	26
	SS error (%)	−3.32	−2.40	−1.86	−1.54	−1.32	−1.16
$L = 0.5893$ m	Nodes	8	9	10	11	12	13
	Total nodes	21	26	29	32	35	38
	SS error (%)	−13.41	−13.20	−12.94	5.20	−6.96	−1.07

Table 7
Relationship between CTFs accuracy and tolerance value.

Tolerance	0.0001	0.001	0.01	0.1
DRF error	−0.57%	−0.92%	−13.86%	−21.71%
Tolerance	0.0000001	0.0001	0.1	0.2
SS error	−0.77%	−0.78%	5.98%	736.69%

Table 8
Relationship between CTFs accuracy and time step.

Time step (s)	900	1200	1800	2700	3600	4800	5400	7200
SS error	−0.18%	−0.26%	−0.34%	−0.47%	−0.77%	−1.08%	−1.56%	−2.43%
FDR error	−0.04%	−0.06%	−0.14%	−0.32%	−0.57%	−1.01%	−1.27%	−2.23%

Table 9
Relationship between CTFs accuracy and frequency range.

$n1$	6	7	8	9	10	10			
$n2$	3					1	2	3	4
FDR error (%)	−0.57	−0.57	−0.57	−0.57	−0.57	−2.11	6.35	−0.57	NaN

Note: NaN is Not a number.

the time step is too large to approximate the temperature variation. Table 8 shows that the CTFs calculation accuracy is not very sensitive to the time step based on wall 24.

- **Frequency points:** This error applies only to FDR method. FDR method estimates a simple polynomial s-transfer function of transient heat conduction in a building construction on the basis of its theoretical frequency characteristics. This simple polynomial s-transfer function is approximately equivalent to the hyperbolic s-transfer function of the total transmission matrix in terms of frequency response characteristics. The concerned frequency range of different slabs is generally different. If the concerned frequency range does not agree with the actual frequency range of the slab, calculation error can be introduced. In FDR method, the frequency response characteristics of the total transmission matrix are calculated within the frequency range $[10^{-n1}, 10^{-n2}]$, which we need to concern [38]. Table 9 indicates that the CTFs calculation accuracy is insensitive to the number $n1$ at all but is very sensitive to the number $n2$. While it is very easy to determine the number $n2$. Calculation accuracy can be well satisfied when the number $n2$ is adjusted from 1 to 4. In general, for lightweight walls, $n1$ is 8, $n2$ is 2; for medium weight walls, $n1$ is 9, $n2$ is 3; and for heavyweight walls $n1$ is 10, $n2$ is 4.

7. Conclusions

Conduction transfer function (CTF) is the numerical solution of the diffusion equation and Fourier's law for transient heat transfer in a building construction. Due to the convenience and ease to implement, CTF method is widely used in building cooling loads and energy calculations. There are a number of methods to calculate CTF coefficients of building constructions, such as DRF, SS and FDR methods, etc. The limitation of methodology possibly results in imprecise or false CTFs. For different material properties and layer number of building constructions, these methods maybe work out CTFs with different precise, and sometimes generating the results without convergence.

In the paper, the calculation principle of three methods is simply introduced. Fourier number and thermal structure factor are introduces to represent the thermal characteristic of the slabs. The heat flux comparison method is presented to verify the accuracy of the CTFs. The test procedure is applied to investigate the applicability of the three methods. ASHRAE wall 19 and 24 are taken as calculating examples. The sources of error in CTF solution are in detail analyzed. The results show that errors for SS and DRF CTF methods are rapidly increasing as $1/(FoS_{ie})$ are increasing. The maximum errors for SS and DRF solutions even reach almost 100%. However, no matter how to change the conditions, FDR method can calculate the CTFs with a very good accuracy, in particular giving good accuracy for very heavyweight constructions. FDR method is more robust and reliable than SS and DRF methods. FDR method is more applicable and practical to calculate CTF coefficients. It may be a better choice to calculating the cooling/heating loads for building structures for the architect/designer.

Acknowledgements

This research work was financially supported by a grant from the Natural Science Foundation of China (NSFC No. 50378033). The authors wish to express their gratitude for this financial support.

References

[1] T. Kusuda, Early history and future prospects of buildings system simulation, in: Proceedings of Building Simulation '99, Kyoto, Japan, 1999.
[2] J. Lebrun, S.W. Wang, Evaluation and emulation of building energy management systems—Synthesis Report, in: IEA (BCS) Annex 17 Final Report, University of Liege, Belgium, 1993.
[3] S.W. Wang, Dynamic simulation of a building VAV air-conditioning system and evaluation of EMCS online control strategies, Building and Environment 34 (1999) 681–705.
[4] Y.M. Chen, J. Zhou, J.D. Spitler, Verification for transient heat conduction calculation of multilayer building constructions, Energy and Buildings 38 (2006) 340–348.
[5] S.W. Wang, Y.M. Chen, Transient heat flow calculation for multilayer constructions using a frequency-domain regression method, Building and Environment 38 (2003) 45–61.
[6] J.D. Spitler, D.E. Fisher, Development of periodic response factors for use with the radiant time series method, ASHRAE Transactions 105 (2) (1999) 491–502.
[7] D.G. Stephenson, G.P. Mitalas, Cooling load calculations by thermal response factor method, ASHRAE Transactions 73 (1) (1967) III1.1–III.1.7.
[8] T. Kusuda, Thermal response factors for multilayer structures of various heat conduction system, ASHRAE Transactions 75 (1) (1969) 246–271.
[9] D.G. Stephenson, G.P. Mitalas, Calculation of heat conduction transfer functions for multilayer slabs, ASHRAE Transactions 77 (2) (1971) 117–126.
[10] G.P. Mitalas, J.G. Arsenault, Fortran IV program to calculate z-transfer functions for the calculation of transient heat transfer through walls and roofs, in: Use of Computers for Environmental Engineering Related to Buildings, Gaithersburg, MD, NBS Building Science Series, vol. 39, 1971.
[11] B.A. Peavy, A note on response factors and conduction transfer functions, ASHRAE Transactions 84 (1) (1978) 688–690.
[12] D.C. Hittle, C.O. Pedersen, Calculating building heating loads using the frequency response of multi-layered slabs, ASHRAE Transactions 87 (2) (1981) 545–568.

[13] LBNL, DOE-2 Engineer manual – Version 2.1A, 1982.
[14] M. Koschenz, Calculation of surface temperature in DOE-2, The Building Energy Simulation User News 20 (2) (1999).
[15] R.K. Strand, F. Winkelmann, W.F.C. Buhl, et al., Enhancing and extending the capabilities of the building heat balance simulation technique for use in EnergyPlus, in: Proceedings of Building Simulation '99, Kyoto, Japan, 1999.
[16] BLAST, Building Loads Analysis and System Thermodynamic, http://www.bso.uiuc.edu/blastmain.htm.
[17] D.C. Hittle, Building Loads Analysis and System Thermodynamic (BLAST) programs, Version 2.0: Users manual, Technical Report E-153, US Army Construction Engineering Research Laboratory (USACERL), 1979.
[18] C. Park, D.R. Clark, G.E. Kelly, HVACSIM+building systems and equipment simulation program: Building loads calculation, NBSIR 86-3331, National Bureau of Standards, 1986.
[19] S.A. Klein, W.A. Beckman, TRNSYS–A transient system simulation program, Solar Energy Laboratory, University of Wisconsin-Madison, Madison, 1994.
[20] R.K. Strand, C.O. Pedersen, D.B. Crawley, Modularization and simulation techniques for heat balance-based energy and load calculation programs: the experience of the ASHRAE Loads Toolkits and EnergyPlus, in: Building Simulation 2001, IBPSA, Rio de Janeiro, 2001.
[21] D.R. Falconer, E.F. Sowell, Electronic tables for the ASHRAE load calculation manual, ASHRAE Transactions 99 (2) (1993) 193–200.
[22] J.E. Seem, Modeling of heat transfer in buildings, Ph.D., University of Wisconsin-Madison, Madison, 1987.
[23] F.C. McQuiston, J.D. Parker, J.D. Spitler, Heating, Ventilating, and Air Conditioning–Analysis and Design, 4th ed., John Wiley & Sons, Inc., New York, 2000.
[24] F.P. Incropera, D.P. DeWitt, Introduction to Heat Transfer, 3rd ed., Wiley, New York, 1996.
[25] ASHRAE, ASHRAE Handbook of Fundamentals, American Society of Heating, Refrigerating, and Air Conditioning Engineering, Inc., 1997.
[26] ASHRAE, ASHRAE Handbook of Fundamentals, American Society of Heating, Refrigerating, and Air Conditioning Engineering, Inc., 2001.
[27] D.C. Hittle, Calculating building heating and cooling loads using the frequency response of multilayered slabs, Ph.D., University of Illinois, 1981.
[28] D.C. Hittle, R. Bishop, An improved root-finding procedure for use in calculating transient heat flow through multilayered slabs, International Journal of Heat and Mass Transfer 26 (1) (1983) 1685–1693.
[29] G.E. Myers, Analytical Methods in Conduction Heat Transfer, McGraw-Hill, New York, 1971.
[30] H.T. Ceylan, G.E. Myers, Long-time solutions to heat conduction transients with time-dependent inputs, International Journal of Heat Transfer 102 (1) (1980) 115–120.
[31] Y. Jiang, State-space method for the calculation of air-conditioning loads and the simulation of thermal behavior of the room, ASHRAE Transactions 88 (2) (1982) 122–138.
[32] K. Ouyang, F. Haghighat, A procedure for calculating thermal response factors of multilayer walls state-space method, Building and Environment 26 (2) (1991) 173–177.
[33] D.M. Wiberg, State-Space and Linear Systems, McGraw Hill Book Company, 1971.
[34] Y.M. Chen, S.W. Wang, Transient heat flow calculation for multi-layer constructions using frequency-domain regression method, Building and Environment 38 (1) (2003) 45–61.
[35] J.D. Spitler, S.J. Rees, D. Xiao, Development of an analytical verification test suite for whole building energy simulation programs-building fabric, ASHRAE 1052-RP final report, American Society of Heating, Refrigerating and Air-Conditioning Engineers, Inc., Atlanta, 2001.
[36] Y.M. Chen, S.W. Wang, Novel Methods for Transient Heat Transfer Analysis of Building Constructions, China Science Press, Beijing, 2004.
[37] E. Kossecka, Relationships between structure factors, response factors, and Z-transfer function coefficients for multilayer walls, ASHRAE Transactions 104 (1A) (1998) 68–77.
[38] Y.M. Chen, S.W. Wang, A new procedure for calculating periodic response factors based on frequency domain regression method, International Journal of Thermal Sciences 44 (2005) 382–392.